This is a preprint, the final version is subject to change, of the American Mineralogist (MSA)
Cite as Authors (Year) Title. American Mineralogist, in press.
DOI: https://doi.org/10.2138/am-2020-7372

Revision 2

Br diffusion in phonolitic melts. Comparison with Fluorine and Chlorine diffusion

Hélène Balcone-Boissard[(1),] Don R. Baker[(2)], Benoit Villemant[(1)], Jean Cauzid [(3)], Georges Boudon[(4)], and E. Deloule[(5)]

(1) ISTEP (UMR 7193)– Sorbonne Université, 4 pl. Jussieu, 75252 Paris, France

(2) Earth and Planetary Sciences, McGill University, 3450 rue University, Montréal, QC, H3A 0E8, Canada

(3) G2R – UMR 7566, Université de Lorraine, BP 70239, 54506 Vandoeuvre-lès-Nancy, France

(4) Institut de Physique du Globe de Paris, Sorbonne Paris Cité, UMR 7154 CNRS, F-75005 Paris, France

(5) Centre de Recherches Pétrographiques et Géochimiques, UMR 7358, CNRS-Université de Lorraine, 54501 Vandoeuvre-lès-Nancy, Cedex, France

Corresponding authors: **Hélène Balcone-Boissard** (helene.balcone_boissard@sorbonne-universite.fr)

Tel : 00 33 1 44 27 51 89

This is a preprint, the final version is subject to change, of the American Mineralogist (MSA)
Cite as Authors (Year) Title. American Mineralogist, in press.
DOI: https://doi.org/10.2138/am-2020-7372

ABSTRACT

Bromine diffusion was measured in two natural phonolitic melts: a K_2O-rich (~10 wt%) one synthesized from the white pumice phase of the 79 AD eruption of Vesuvius (Italy) and a Na_2O-rich (~10 wt%) one corresponding to the most differentiated melt of the 12 000 BC eruption of the Laacher See (Germany). Experiments were performed at 0.5 and 1.0 GPa, 1250 to 1450 °C, at anhydrous and hydrous (2.65 +/-0.35 wt% of dissolved water) conditions. Experiments conducted with the diffusion-couple technique in the piston cylinder were performed with only bromine diffusing and with the simultaneous diffusion of a halogen mixture (F, Cl, Br) in order to evaluate the interactions between the halogens during diffusion. The diffusion profiles of Br were measured by X-Ray fluorescence using synchrotron radiation microprobe (SYXRF), ID18F, at the European Synchrotron Radiation Facility (ESRF, France). Bromine diffusion displays Arrhenian behaviour under anhydrous conditions that is similar when it diffuses alone and when it diffuses with F and Cl. The Br diffusion coefficients range between 2 x 10^{-12} m²/s at 1250 °C and 1.5 x 10^{-11} m²/s at 1450 °C for the Na-rich melt and between 3 x 10^{-12} m²/s at 1250 °C and 2.5 x 10^{-11} m²/s at 1450 °C for the K-rich melt, at 1.0 GPa. Although Br mobility is independent of F and Cl in anhydrous phonolitic melts, its behaviour may be dependent on the dominant alkali in the melt, as previously observed for Cl, but not F. For hydrous experiments, although the data are scattered, the Br diffusivity increases a slighlty with water and the Na/K ratio seems to influence Br diffusivity. Similarly to noble gases, halogen diffusivity at a given temperature in the phonolitic melts appears related to the ionic porosity of the silicate structure. Compared to basaltic melt, Br diffusivities are approximately one order of magnitude lower in the Na-

42 phonolite melt, because of the difference of the pre-exponential factor. Considering the results
43 here, Br mobility appears to be decoupled from melt viscosity.

44 Keywords: Bromine, phonolite, diffusivity, ionic porosity, alkali

45

46 **INTRODUCTION**

47 Volatiles play a significant role in igneous processes; they not only affect magma
48 properties (e.g., viscosity) and therefore transport in magmatic conduits, but also influence
49 diffusion and bubble growth rates, possibly leading to dramatic explosive eruptions. Among the
50 volatiles, halogens (F, Cl, Br, I) have received increasing attention in recent years, despite their
51 low abundances on Earth (e.g., Aiuppa et al. 2009). In addition, determination of halogen
52 distributions and the geochemical processes controlling their mass transfer between solid and
53 fluid reservoirs on Earth are relevant since they can be used to address many significant questions
54 in various geoscience fields of research (Hanley and Koga 2018), such as the source and
55 evolution of hydrothermal fluids and the role they play in ore deposit formation, metamorphic
56 processes, the reconstruction of marine sedimentary paleo-environments, and the tracking of
57 mantle-to-crust mass transfer associated with subduction (Shinohara et al. 1989; Carroll and
58 Webster 1994; Aiuppa et al. 2009; Baker and Balcone-Boissard 2009; Webster et al. 2009;
59 Vigneresse 2009; Lecumberri-Sanchez and Bodnar 2018). Moreover, halogens exert a significant
60 influence on the physico-chemical properties and the structure of silicate melts (Manning 1981;
61 Mysen and Virgo 1985; Webster et al. 1989; Webster and Holloway 1990; Mysen et al. 2004;
62 Dalou et al. 2015; Grousset et al. 2015; Webster et al. 2018).

63 Halogens are incompatible (lithophile) elements during mineral-melt partitioning and
64 behave as volatile elements. With decreasing ionic size from I- to F-, halogen anions describe an

increasing energy of formation for NaX (where X is a halogen) salts, increasing short-range order in glasses with modifier cations such as Na, K and Ca (Luth 1988; Zeng and Stebbins 2000; Louvel et al. 2020), and increasing volatility and solubility. Halogen diffusivity in silicate melts is of particular interest because the differences between the diffusivity of water, halogens, and sulfur appear to be significant enough on the basis of the published data (Alletti et al. 2007; Balcone-Boissard et al. 2009; Feisel et al. 2019) that during melt inclusion entrapment (Baker 2008), or during rapid bubble or crystal growth, diffusive fractionation between water and the halogens, and between halogens and sulfur, are expected to occur. The diffusive fractionation between halogens in melts has further bearing on the monitoring of volcanic activity, and may especially be used as a volcanic eruption precursor supported by the development of routine halogen mesurements in volcanic gases and plumes. (Bobrowski et al. 2003; Gutman et al. 2018 for a review). Though diffusive processes operate at a limited, local scale, they can modify the composition of gases, melts and even crystals (Smith et al. 1955). Although Br is less abundant than Cl in silicate melt, it is known to be about two orders of magnitude more efficient than chlorine in destroying stratospheric ozone (Daniel et al. 1999; McElroy et al. 1986). Thus, we need to fill the gap in our knowledge concerning the diffusivities of halogens in silicate melts and better understand the link between Br concentrations in melts and the amount released in atmosphere, because Br is an ozone-destroying agent (Bobrowski et al. 2003).

Little is known about halogen diffusion in magmatic melts. The few published studies (Bai and Koster van Groos 1994; Alletti et al. 2007; Balcone-Boissard et al. 2009; Böhm and Schmidt 2013; Yoshimura 2018; Feisel et al. 2019) demonstrated that the diffusion of halogens display Arrhenian behaviour at magmatic temperatures and found no influence of halogen concentration on their diffusivity. However, currently no data exists on iodine diffusion. Little is

known about Br behaviour in silicate melt in general (Bureau and Métrich, 1992, 2003; Bureau et al;, 2000; Cadoux et al., 2018; Balcone-Boissard et al., 2010; Villemant et al., 2017; Fusswinkel et al., 2018).

We performed a series of bromine diffusion experiments using the diffusion couple technique, on dry and hydrous phonolitic melts of the K-rich, 79 AD Vesuvius eruption, as well as similar experiments on a Na-rich phonolite from the 12 000 BC Laacher See eruption (Germany). The diffusion profiles of Br were measured by X-Ray fluorescence using synchrotron radiation microprobe (SYXRF), ID18F, at the European Synchrotron Radiation Facility (ESRF), France. These compositions are not only important because of these two classic eruptions, but also because they represent some of the most halogen-rich magmas known (Balcone-Boissard, 2008). The experimental temperatures ranged between 1250 and 1450 °C, at 1.0 GPa under anhyrous and hydrous (~2.65 wt.% water) conditions; we also performed anhydrous experiments at 1200 and 1250 °C, and 0.5 GPa, to investigate the effect of pressure on diffusion. These experimental conditions allow us to apply our bromine diffusion results to temperatures and pressures of crustal magma chambers and expand our understanding of volatile transport in magmatic systems.

EXPERIMENTAL AND ANALYTICAL TECHNIQUES

Experiments were performed to determine Br diffusivity in the two natural phonolitic melts (Vesuvius 79 AD and Laacher See 12000 BC) previously used for F and Cl diffusion measurements in Balcone-Boissard et al. (2009). Nearly volatile-free and chemically homogeneous starting materials were obtained by fusing ground powders of the natural glasses at 1400 °C and 1 atm; ion microprobe analysis yielded Br concentrations below 5 ppm in these

glasses (Table 1) and water concentrations in these glasses are expected to be approximately 1000 ppm based upon the work of Dixon et al. (1995) on basaltic melts. Fused glasses were then ground for 40 minutes in an agate mortar to obtain a powder with grains below 50 µm in size.

To produce Br-enriched starting glass powders we chose two aliquots of the volatile-free powdered glass and added 8000 ppm of Br as a NaBr salt. A second starting material consisted of volatile-free powdered glass with a mixture of NaF-NaCl-NaBr in the same concentrations (i.e. ~ 5000 ppm of each salt). In order to homogenize each mixture, the powders were ground under ethanol in an agate mortar for 1 h, before being dried at 400 °C for at least 2 h. We then fused an aliquot of each mixture at 1.0 GPa, 1400 °C for 2 h in a graphite capsule in a piston-cylinder apparatus, using an NaCl-pyrex-crushable alumina assembly (Baker 2004). Br concentrations were determined by secondary ion mass spectrometry (SIMS) following the method described in Cadoux et al. (2017): the Br-only and halogens mixture glasses contain 8000 and 5000 ppm Br, respectively..

In order to study the role of dissolved water we produced hydrous glasses by adding either ~2 or ~5 wt% distilled water to the glasses and fused them again in graphite capsules inside welded Pt capsules at 1250 °C – 1.0 GPa for 4 h. To minimize H_2O loss, the free space between the Pt capsule and the crushable alumina cylinder of the piston-cylinder assembly was filled with packed pyrophyllite powder. The final hydrated glass has 2.3 ± 0.02 wt% for Laacher See composition and 3 ± 0.1 wt% for Vesuvius composition (analysed by SIMS). The homogeneity of the water concentration in the diffusion couple is demonstrated by traverses performed along the diffusion-couple by SIMS (Supplementary material S1).

The anhydrous diffusion experiments were conducted simultaneously for Br and for the F-Cl-Br mixture, with an experimental design similar to Baker (2004). The diffusion couple was

constructed by drilling 4 cylindrical holes (1.6 mm diameter, 5mm long) in a 6 mm diameter graphite cylinder. The Br-enriched phonolitic glass (i.e. NaBr or the NaF-NaCl-NaBr mixture) was first packed into the lower halves (2 mm) of each hole and the top halves (2 mm) were filled with the corresponding Br-free phonolitic glass. The last 1 mm was backfilled with graphite powder. The graphite cylinder was then capped by a graphite plug (1 mm thick).

The hydrous diffusion experiments used graphite capsules (1 mm inner diameter, 4 mm long) inside welded Pt capsules; Br-bearing and Br-free materials used in the diffusion couple were both hydrated and the graphite capsules filled the same way as for the anhydrous experiments. Two capsules were placed in each assembly in order to simultaneously perform diffusion experiments for the two different phonolitic compositions at the same water concentrations and identical temperature and pressure conditions.

Diffusion experiments were performed in a piston-cylinder apparatus with 19.1 mm NaCl-pyrex-crushable alumina assemblies. A summary of experimental conditions can be found in Table 2.Temperatures were measured with Type C thermocouples. The run procedure consisted of simultaneously pressurizing and heating the assembly. For the synthesis experiments two heating rates of 100 °C/min until 100 degrees below the run temperature and 50 °C/min for the final 100 °C up to the run temperature were used. For diffusion experiments, a single heating rate of 100 °C/min was preferred and resulted in less than 5 °C overshoot of the run temperature. All experimental durations (between 400 and 4500 s) are calculated based upon the time the experiment reached the desired run temperature. At the end of each experiment the samples were quenched isobarically at 100 °C/s down to 600 °C. After quenching, the samples were embedded in epoxy, ground open, and polished for Br analyses.

The SEM system used to investigate the run products here was a Zeiss Supra 55 VP (ISTeP – Sorbonne Université – Paris), with a Brucker-Quad EDS detector. The resolution was 125 eV for a current of 35-40 nA, a voltage of 15 keV for the chemical mapping of 1024x2048 pixels (256 µs/point of resolution with 15 frames). The SEM images using backscattered electron (BSE) were obtained at 15 keV and with a current of 10 nA.

The diffusion profiles of Br were measured by X-Ray fluorescence using synchrotron radiation microprobe (SYXRF), ID18F, at the European Synchrotron Radiation Facility (ESRF), France. A double crystal monochromator using Si (111) crystals was set to produce a beam of 28 keV X-rays and the secondary X-rays detected by a Si(Li) detector (Somogyi et al. 2001) placed at 90° to the incident beam in the polarization plane to minimize scattering. The beam was focused with Compound Refractive Lenses onto the sample in a rectangular spot of 2 x 8 µm. The spot size was determined by the knife-edge technique using a thin gold test-object. We analyzed between 120 and 160 points per profile, with a 10 s counting time for each point and a step between 20 and 30 µm depending the run. We also analyzed profiles with a 30 s counting time for each point but there was no improvement in the sensitivity. The Br diffusivity was calculated from the diffusion profile obtained after extraction of the intensity of the Br peaks using PyMca software for peak fitting. No absolute calibration of the Br concentration was necessary for this study because the SYXRF data were collected on an homogeneous sample (no change of density) with a fixed geometry from the source to the fluorescence detector. All measurements are given as the integrated area under the bromine peak (Fig. 1). In some cases, two traverses were performed along the same diffusion profile to estimate the diffusion coefficient (Table 2). The data allow us to estimate the activation energy that represents the energy required to activate atoms to a condition in which they can undergo diffusive transport.

The activation energy is usually represented by the symbol Ea in Arrhenius equations for the diffusion coefficient, D = Do exp(−Ea/RT), with Do being the pre-exponential factor deduced from Arrhenius law, commonly associated with the jump distance of an ion during diffusion (Shewmon 1963).

RESULTS

Br diffusivity in phonolitic melt

After polishing, the run products were analyzed optially in reflected light and using the scanning electron microscope. No microlites (<1 vol.-%) were found in the run products and no vesicles were found within the glass using both optical microscopy and the scanning electron microscope.

Although Br might be lost from the graphite capsules used in the anhydrous experiments, there is no evidence that this occurred, as based upon three observations. The first observation is that the high-concentration ends of the diffusion profiles are flat and are similar in anhydrous experiments in graphite capsules and hydrous experiments in graphite-lined, sealed Pt capsules (Fig. 1); such an observation is inconsistent with loss of Br from the graphite capsules. The second observation is that the diffusion profiles were well fit by interdiffusion of Br between the Br-enriched and Br-depleted halves of the experiments. If additional diffusive loss would have occurred, then such good fits would not be expected. The third observation is that multiple analytical traverses yielded the same calculated diffusion coefficients; such a similarity would not be expected if Br loss occurred along the circumference of the graphite capsules.

In order to investigate the possibility of convection at the interface between the two glasses, some chemical maps using the scanning electron microscope were performed on the

zero-time experiment with Laacher See and an anhydrous experiment (at 1450 °C) for Vesuvius (See supplementary material S3). No evidence of convection was found.

For the hydrous experiments, we investigated the possibility that water diffusion occurred during halogen diffusion. A water concentration profile was performed on the 4 experiments at 1450 °C to ensure that no H_2O diffusion occurred. The flat, nearly homogeneous profiles for total water in two experiments demonstrates that Br diffusion occurred in melts of constant water concentration (see supplementary material S1).

One «zerotime» experiment was performed at 1350 °C for the mixture with 2.3 ± 0.02 wt% of water for Laacher See composition and 3 ± 0.1 wt% for Vesuvius composition in order to investigate the extent of diffusion during heating to the highest experimental temperature. Although diffusion occurred during heating, its extent was minor and does not affect the diffusivities measured in the experiments.

Calculation of bromine diffusion coefficients from concentration profiles

We applied the procedure for calculating Br diffusion previously used for F and Cl diffusivity measurements (Balcone-Boissard et al. 2009). We fit the measured diffusion profiles (e.g., Fig. 1) using a non-linear curve-fitting program developed to fit diffusion between two semi-infinite media (Crank 1975):

$$C(x, t) = (C_{low}+C_{high})/2 + (C_{low}-C_{high})/2 \times \mathrm{erf}((x - x_0) / (2\sqrt{Dt})),$$

where C(x, t) is the concentration along the diffusion profile plotted in a concentration vs. distance diagram, x is the distance along the profile (in meters) and t is the experimental duration (in seconds). C_{low} and C_{high} are respectively the halogen concentrations in the depleted and the enriched semi-infinite media that make up the diffusion couple, expressed here as the mean Br

values of the plateaus; x_0 represents the centre of the diffusion profile, at the interface between the two melts along the diffusion profile, and D is the diffusion coefficient or diffusivity.

All diffusion profiles were well fit by the above equation. The fit of the diffusion profiles using a single diffusivity confirms that the diffusion coefficient of bromine is independent of the bromine concentration over the range investigated, as already highlighted for F and Cl (Baker and Balcone-Boissard 2009), although we note that the Br concentrations used here largely exceed that found in nature. The comparison of the diffusion coefficients measured in two experiments that only differ by experimental duration demonstrate that the measured diffusion coefficients of Br were not affected by experimental duration, which indicates that diffusion was the sole transport mechanism in these experiments (Fig. 1; Table 2).

The diffusion coefficients for both K-rich and Na-rich phonolitic melt compositions are summarized in Table 2, with maximum uncertainties estimated at ± 20%. This estimate is based upon experiments of different durations at the same conditions, modelling of duplicate diffusion profiles from the same experiment, and Monte Carlo uncertainty analysis simulations (Alletti et al. 2007). As previously observed for F and Cl in the same melt compositions, the bromine diffusion coefficients increase with increasing temperature (Figs. 2, 3; Table 2, 3).

Effect of temperature, pressure and mixed halogens on diffusion

At anhydrous conditions, diffusion coefficients for Br range between 1.9 – 2.3 x 10^{-12} m²/s at 1250 °C and 1.5 x 10^{-11} – 9.2 x 10^{-12} m²/s at 1450 °C for the Na-rich melt and between 2.8 - 3.2 x 10^{-12} m²/s at 1250 °C and 2.5 x 10^{-11} m²/s at 1450 °C for the K-rich melt. Bromine displays Arrhenian behaviour under anhydrous conditions (Fig. 2). Diffusion experiments using a halogen mixture of F, Cl and Br were performed at dry conditions over the same range of temperatures

(1250 to 1450 °C) and at the same pressure (1.0 GPa) as the Br-only diffusion experiments (results for F and Cl in these experiments were previously reported in Balcone-Boissard et al. 2009). For the studied melt compositions, there was no significant difference in the diffusion coefficient measured in experiments involving only Br or containing the F-Cl-Br mixture (Fig. 2, Table 2a). Br diffusivities in both types of experiments (with only Br and with the mixture) were combined to calculate the Arrhenius parameters. Best fit parameters values for the Arrhenius equations are reported in Table 3. At anhydrous conditions the activation energy for Br diffusion is 118 kJ/mol in the K-phonolite and 161 kJ/mol in the Na-phonolite (Table 3).

In order to investigate the effect of pressure on halogen diffusion in anhydrous melts, anhydrous experiments at 0.5 GPa, 1250 °C were performed for melts with the halogen mixture (Table 2a). No significant effect of pressure on Br diffusivity was observed in the pressure range investigated for both compositions (D^{Br} at 1250 °C is ~3 x 10^{-12} m²/s at 0.5 or 1.0 GPa for the Na-rich melt, and D^{Br} at 1250 °C is ~2.9 x 10^{-12} m²/s at 0.5 or 1.0 GPa for the K-rich melt).

The effect of water on Br diffusion

Br diffusivity under hydrous conditions (with 2.65 +/- 0.35 wt% H_2O) was only investigated using the F-Cl-Br mixture. The diffusion coefficients of both K-rich and Na-rich phonolitic melts for hydrous experiments are compiled in Table 2b. For these hydrous experiments only 3 temperatures were investigated. These few experiments are not well-enough constrained to claim robust findings, but provide a general tendency that needs to be confirmed in order to have more precise diffusion coefficients and Arrhenius equations.

The addition of water was expected to enhance Br diffusivity in all phonolitic melts, as previously seen for F and Cl in both melts studied. Here the first results suggest that water has a

small, enhancing effect on Br diffusion in phonolitic melts. The effect of adding water to the K-phonolitic melt results in only a modest decrease in Br diffusion activation energy to 99 kJ/mol and an apparent increase in activation energy in the Na-phonolitic melt to 189 kJ/mol (Table 3). However in both cases the activation energies are within uncertainty of those for Br diffusion in the respective anhydrous melts, as are the D_o values.

DISCUSSION

Br diffusion mechanisms in anhydrous melts

One aim of this study was to investigate the influence of the dominant alkali cation (Na or K) on Br diffusivity in phonolitic melts, following previous results for F and Cl that demonstrated that the dominant alkali affect Cl but not F diffusivity (ie., Cl diffusivity is higher in K-rich phonolites) (Balcone-Boissard et al. 2009).We attributed this observation to strong K-Cl interactions in the melt (Balcone-Boissard et al. 2009). Br diffusivity in both anhydrous phonolitic melts is similar over the temperature range investigated (Fig. 2), however the activation energy for Br in the K-phonolite is significantly lower than in the Na-phonolite. This would lead to higher Br diffusivity in the K-phonolite relative to the Na-phonolite at lower temperatures. This behaviour suggests that Br mobility may be dependent on the dominant alkali in the melt, as observed for Cl, but not F, in the same melts (Balcone-Boissard et al. 2009).

The bromine diffusivity measured in the phonolites of this study can be compared against that measured in an Etna basalt by Alletti et al. (2007) (See supplementary material S4). Interestingly, the activation energy for Br diffusion in the Na-phonolitic melt and in the basaltic melt of Alletti et al. (2007) are similar, both approximately 180 kJ/mol. (Note that we

recalculated the activation energy in the anhydrous basalt by combining all of the anhydrous Br diffusion measurements in the run table of Alletti et al. 2007.) However, the Br diffusivities in the basaltic melt are approximately one order of magnitude higher than in the Na-phonolite due to its higher pre-exponential factor. On the other hand, the activation energy for Br diffusion in the K-phonolite is much lower, ~ 122 kJ/mol.

The comparable activation energies for Br diffusion in the Na-phonolite and basalt (whose dominant alkali is also Na) melts imply that the energetics of breaking and reforming of bonds (Henderson et al. 1985), and possibly the average atomic coordination of Br are similar in both melts, but different from that in the K-phonolite melt. These energetic differences are consistent with a shorter, stronger bond between Na-Br than between K-Br and provide evidence that bromine is complexed with alkalis in the melt structure, not randomly substituted for oxygen (Widdifield et al. 2009; Louvel et al. 2020), except for some data at high pressure (up to 7.6 GPa, Cochain et al. 2015) that suggest bonding between Br and cations in the melt, in particular with Na and less with O. This mechanism is expected to be dependent on silicate melt composition (Mysen and Richet, 2019).

The Br diffusivity appears to be decoupled from melt viscosity, which has been demonstrated to couple with Si-Al interdiffusion in intermediate to silicic melts through the Eyring equation (Baker 1990). For example, the viscosity of the anhydrous Na-phonolite and the K-phonolite were calculated at 1350 °C to be 720 and 1350 Pa s following Giordano et al. (2008); these viscosities combined with the Eyring equation would lead to a factor two difference in diffusivity, which is not seen in the measurements. The low viscosity of the basalt used by Alletti et al. (2007), 6 Pa s, would lead to a 100-fold increase in the Br diffusivity when compared to the Na-phonolite, but only a 10-fold increase is seen. This decoupling of Br

317 diffusion with viscosity is similar to the decoupling of alkali diffusion and viscosity (Jambon and
318 Semet 1978; Lowry et al. 1982; Henderson et al. 1985; Baker 1990) and would be consistent with
319 alkali-Br complexes in the melt that link the Br diffusivity to that of alkalies, although the former
320 is orders of magnitude lower than the latter.

321 The mobility of halogens at a given temperature in the phonolitic melts is related to their
322 ionic properties (radius and charge). The ionic radii of halogens increase with increasing atomic
323 number: 133, 181 and 198 pm for F, Cl and Br respectively. Figure 4 demonstrates that halogen
324 diffusivity in phonolitic compositions is a function of the ionic radius and describes a continuous
325 negative correlation with ionic radius when Br is added to the previous data obtained on F and Cl
326 (Balcone-Boissard et al. (2009). Comparison of Br, F, and Cl diffusion in these two phonolitic
327 melts demonstrates similar behaviors. Fluorine always displays the highest diffusivity,
328 approximately 1 order of magnitude above Cl and Br.

329 The correlation between ionic radius and diffusivity is similar to that seen for the
330 neighbouring noble gases in the periodic table, but contrasts with diffusion seen for halogens in
331 basaltic melts, which are independent of the ionic radius (Alletti et al., 2007). For noble gases,
332 the accepted mechanism for their diffusion in silicate melt is dependent upon the ionic porosity
333 (Lux, 1987), that is the difference between the unit cell volume of a silicate structure and the
334 calculated volume of the anions and cations, which means that it is a measure of the integrated
335 "free" space in the silicate melt (Carroll and Stolper 1993). Following this definition, lower
336 density, polymerized melts (such as phonolitic melts) exhibit a high ionic porosity, in contrast to
337 higher density, depolymerized melts (such as basaltic melts). Similarly to what is observed for
338 noble gases, we expect that the ionic porosity influences halogen mobility within phonolitic

339 melts; Br, the largest halogen here studied, should be the halogen most sensitive to ionic porosity
340 changes.

341 We hypothesize that as melt compositions change from silicic to basaltic and the ionic
342 porosity decreases, the larger free space ("holes") in the melt structure suitable for Br diffusion
343 become less common, and therefore separated by greater distances, than smaller "holes". This
344 hypothesis is consistent with the larger D_o value, commonly associated with the jump distance of
345 an ion during diffusion (Shewmon, 1963), in the Arrhenius equation for Br diffusion in a basaltic
346 melt, ~2 x 10^{-5} m^2s^{-1} (Alletti et al., 2007) than in the Na-phonolite, ~2 x 10^{-6} m^2s^{-1}. Even though
347 the Br activation energies are similar in both melts (basaltic and Na-phonolitic), because the D_o
348 value of basalt is higher than Na-phonolite each diffusive "jump" of a Br ion is greater, and the
349 net result is that Br diffusivity in the basaltic melt is higher than in Na-phonolitic melt at typical
350 magmatic temperatures. This hypothesis also implies that the K-phonolite, with a D_o value 3
351 orders of magnitude below that of the Na-phonolite should have even more, closely spaced
352 "holes" in the melt structure suitable for Br diffusion.

353 Investigations of the Br environment in silicate melts of magmatic interest are still few In
354 addition, the lack of any viscosity-diffusivity relation and the failure of Eyring equation in
355 phonolitic and basaltic melts implies no significant link of Br with the silicate network of silicon
356 and oxygen atoms. Br may consequently display multiple behaviours and bonding to Na, K and
357 Ca ions (Louvel et al., 2020).

358 **Influence of H_2O**

359 Our preliminary Br diffusion results on hydrous melts demonstrate little effect of water on Br
360 diffusivity. The activation energies of Br diffusion in hydrous and anhydrous phonolitic melts
361 are within uncertainty of each other and the D_o values change by less than an order of magnitude.

These D_o values for the hydrous melts are poorly constrained and may be the same as in anhydrous melts. Such small changes in Br diffusivity with addition of water further underscore the lack of correlation between Br diffusion and melt viscosity because the phonolitic melts with 2.65 wt% water are expected to have viscosities of only ~ 20 Pa s (calculated following Giordano et al. 2008). As discussed above for anhydrous melts, the decoupling of alkali diffusion from melt viscosity has also been observed, leading us to hypothesize that large alkali ions and large halogen anions diffuse by similar mechanisms in the melts studied. This result implies that we can use the anhydrous diffusivities to model melts with up to ~ 2.65 wt% water with reliability.

IMPLICATIONS

Our study demonstrates different effects of Na and K on Br diffusion in phonolitic melts. By comparison to halogen diffusion in silicic melts (rhyodacitic melt, Feisel et al. (2019), without Br) and in basaltic melts (Alletti et al. (2007)-including Br), the diffusion measurements for Br confirm the influence of melt composition on diffusivity. Also importantly, Br diffusivity appears to be decoupled from melt viscosity. Similarly to noble gases, halogen diffusivity at a given temperature in the phonolitic melts seems to be related to the ionic porosity (radius and charge) of the silicate structure. Those results highlight that more effort is needed on halogen solubility mechanisms.

Combined with our previous one (Balcone-Boissard et al. 2009), this study provides the fundamental measurements needed to better characterize halogen (F, Cl, Br) behaviour in silicate melts, which is of prime importance to understand halogen content and mobility in igneous processes. Diffusive fraction during rapid growth of crystals or bubbles has previously been modeled to evaluate its effect on the modification of halogen ratios in exsolved fluids and

385 minerals (e.g., Alletti et al. 2007; Balcone-Boissard et al. 2009, 2010). The extent of any possible
386 diffusive fractionation between elements is a function of their partition coefficients and diffusion
387 coefficients, which can lead to significant variations in the ratios of elements at the interfaces and
388 therefore influence the compositions of the growing phases. Modeling can be used to evaluate
389 the extent of possible diffusive fractionation in phonolitic melts and compared with studies of
390 rock and gas samples in order to better understand the storage and transport of halogens in
391 magmatic systems.

392 As an example of possible diffusive fractionation, we consider the study of Wang et al. (2014)
393 who investigated the halogen variations in volcanics of the Upper Rhine Graben and demonstrate
394 that Cl/Br ratios remain relatively constant (371 ± 120), whereas the F/Cl ratios vary from < 0.1
395 in the evolved (low Mg-number) phonolitic samples to ~ 100 in the primitive (high Mg-number)
396 mafic ones. Although much of the variation in the F/Cl ratio is probably due to their differing
397 partitioning between melts and fluids or crystals (Wang et al. 2014), some could be due to
398 diffusive fractionation during volatile exsolution and degassing. Complete understanding of
399 halogen behavior in magmatic systems requires that we understand the relative roles of
400 equilibrium partitioning and diffusive fractionation in producing the final concentrations in rocks
401 and modeling their outgassing into the atmosphere.

402 The experimental diffusivities of Br, Cl and F in hydrous Laacher See melts studied here and in
403 Balcone-Boissard et al. (2009), which was collected from the Upper Rhine Graben, (Fig. 5)
404 demonstrate that at magmatic temperatures between 1000 to 1200 °C the diffusivities of Br and
405 Cl are similar and little diffusive fractionation should occur, whereas the diffusivity of F is
406 significantly higher than Cl. At these conditions, diffusive fractionation could be partially
407 responsible for variations in the F/Cl ratio while little-affecting the Br/Cl ratio. At temperatures

below 1000 °C the diffusivities and Cl and Br begin to diverge significantly because of their differing activation energies and diffusive fractionation between these elements becomes possible in vesiculating, or rapidly crystallizing, phonolitic melts. Thus, any diffusive fractionation between halogens will be greater at low temperature. Diffusive fractionation between halogens on active volcanic system may thus be interesting to monitor as potential volcanic eruption precursors for volcanic hazard forecasting (e.g. Aiuppa et al. 2009). In addition, multi-species volatile diffusion in melt embayments or zoned melt inclusions may also serve as a chronometer to retrieve timescales that reflect magma ascent on the order of minutes to days prior to eruption.

Acknowledgments

We are grateful to G. Wörner for providing the Laacher See starting material, Lang Shi for microprobe measurements in Montreal and M. Fialin and F. Couffignal in Paris. R. Kalsi is thanked for writing the computer program to reduce the data and calculate the diffusion coefficient.

References

Aiuppa A., Webster J.D., and Baker D.R. (2009) Halogens in volcanic systems. Chemical Geology 263, 1-18.

Alletti M., Baker D.R., and Freda C. (2007) Halogen diffusion in a basaltic melt. Geochimica et Cosmochimica Acta 71, 3570-3580.

Bai T.B. and Koster van Groos A.F.(1994) Diffusion of chlorine in granitic melts. Geochimica et Cosmochimica Acta 58, 113–123.

Baker, D.R. (1990) Chemical interdiffusion of dacite and rhyolite: anhydrous measurements at 1 atm and 10 kbar, application of transition state theory, and diffusion in zoned magma chambers. Contributions to Mineralogy and Petrology 104, 407-423.

Baker D.R. (2004) Piston-cylinder calibration at 400 to 500 MPa: A comparison of using water solubility in albite melt and NaCl melting. American Mineralogist 89, 1553-1556.

Baker D.R. (2008) The fidelity of melt inclusions as records of melt composition. Controbutions to Mineralogy and Petrology, 156(3):377-395.

Baker D.R. and Balcone-Boissard H (2009) Halogen diffusion in magmatic systems: Our current state of knowledge. Chemical Geology 263 (1-4), 82-88

Balcone-Boissard H., Baker D.R., Villemant B., and Boudon G. (2009) F and Cl diffusion in phonolitic melts: Influence of the Na/K ratio. Chemical Geology 263, doi:10.1016/j.chemgeo.2008.08.018.

Balcone-Boissard H. (2008). Le comportement des éléments halogènes au cours du dégazage des magmas en relation avec leur chimie et le style éruptif, 332 p. PhD thesis, University Paris7, Paris.

Balcone-Boissard H., Villemant B. and Boudon G. (2010), Behavior of halogens during the degassing of felsic magmas. Geochemistry Geophysics Geosystem, 11, Q09005, doi:10.1029/2010GC003028.

Bobrowski N., Honninger G., Galle B., and Platt U. (2003) Detection of bromine monoxide in a volcanic plume. Nature 42, 273-276.

Böhm A. and Schmidt, B.C. (2013) Fluorine and chlorine diffusion in phonolitic melt. Chemical Geology , 346, 162–171.

Bureau H., and Métrich N. (1992) An experimental study of bromine behaviour in water-saturated silicic melt. Geochimica et Cosmochimica Acta 67(9), 1689-1697

Bureau H., Keppler H.and Métrich N. (2000) Volcanic degassing of bromine and iodine: experimental fluid/melt partitioning data and applications to stratospheric chemistry. Earth and Planetary Science Letters, 183, 51–60.

Bureau, H., Métrich, N., 2003. An experimental study of bromine behaviour in water saturated silicic melts. Geochimica et Cosmochimica Acta 67, 1689–1697.

Cadoux A., Iacono-Marziano G., Scaillet B., Aiuppa A., Mather T. et al. (2018) The role of melt composition on aqueous fluid vs. silicate melt partitioning of bromine in magmas. Earth and Planetary Science Letters, Elsevier, 498, pp.450-463.

475 Cadoux A., Iacono-Marziano G., Paonita. A., Deloule E., Aiuppa A., Eby N., Costa M., Brusca
476 L., Berlo K., Geraki K., Mather T.A., Pyle D.M., and Di Carlo I. (2017) A new set of
477 standards for in-situ measurement of bromine abundances in natural silicate glasses :
478 application to SR-XRF, LA-ICP-MS and SIMS techniques, Chemical Geology, doi :
479 10.1016/j.chemgeo.2017.01.012.
480
481 Carroll, M. R., and Webster, J. D. (1994) Solubilities of sulfur, noble gases, nitrogen, chlorine,
482 and fluorine in magmas. Reviews in Mineralogy, 30, 231-279.
483
484 Carroll, M.R., and Stolper E.M. (1993) Noble gas solubilites in silicate melts and glasses : New
485 experimental results for argon and the relationship between solubility and ionic porosity.
486 Geochimica et Cosmochimica Acta 57, 5039-5092.
487
488 Cochain B., Sanloup C., de Grouchy C., Crépission C., Bureau H., Leroy C., Kantor I. and
489 Irifune T. (2015) Bromine speciation in hydrous silicate melt at high pressure. Chemical
490 Geology, Elsevier, 2015, 404, pp.18-26. ⟨10.1016/j.chemgeo.2015.03.015⟩. ⟨hal-
491 01136078⟩
492
493 Crank J. (1975) The Mathematics of Diffusion. Clarendon-Oxford, London.
494
495 Dalou C., Mysen B.O., and Foustoukos D. (2015) In-situ measurements of fluorine and chlorine
496 speciation and partitioning between melts and aqueous fluids in the Na2O-Al2O3-SiO2-
497 H2O system. *American Mineralogist* ; 100 (1): 47–58. doi: https://doi.org/10.2138/am-
498 2015-4859
499
500 Daniel J. S., Solomon S., Portmann R.W., and Garcia R. R. (1999) Stratospheric ozone
501 destruction: The importance of bromine relative to chlorine. Journal of Geophysical
502 Research 104, 23871–23880.
503
504 Dixon JE, Stolper EM, and Holloway JR (1995) An experimental study of water and carbon
505 dioxide solubilities in Mmd-ocean ridge basaltic liquids. Part I: calibration and solubility
506 models. Journal of Petrology 36(6) 1607-1631.
507
508 Feisel Y., Castro J.M., and Dingwell D.B. (2019) Diffusion of F and Cl in dry rhyodacitic melt.
509 *American Mineralogist* ; 104 (11): 1689–1699. doi: https://doi.org/10.2138/am-2019-7095
510
511 Fusswinkel T., Giehl C., Beermann O., Fredriksson J.R., Garbe-Schönberg D., Scholten L. and
512 Wagner T. (2018) Combined LA-ICP-MS microanalysis of iodine, bromine and chlorine
513 in fluid inclusions. Journal of Analytical Atomic Spectrometry, 33, pp. 768-783
514
515 Giordano D., Russell J.K., Dingwell D.B. (2008) Viscosity of Magmatic Liquids: A Model. Earth
516 and Planetary Science Letters 271, 123–134
517
518 Grousset L., Pili E., Neuville D.R. (2015) Incroportation et rôle des halogènes dans les silicates
519 vitreux fondus. Materiaux et Techniques 103, (405). DOI: 10.1051/mattech/2015040
520

Gutmann A, Bobrowski N, Roberts TJ, Rüdiger J and Hoffmann T (2018) Advances in Bromine Speciation in Volcanic Plumes. Frontiers of Earth Sciences 6:213. doi: 10.3389/feart.2018.00213

Hanley J.J. and Koga K.T. (2018) Halogens in Terrestrial and Cosmix Geochemical Systems: Abundances, Geochemical Behaviors and Analytical Methods. In The Role of Halogens in Terrestrial and Extraterrestrial Geochemical Processes, Springer Geochemistry, D.E. Harlov and L. Aranovich (eds.). https://doi.org/10.1007/978-3-319-61667-4_2.

Henderson P., Nolan J., Cunningham G.C., and Lowry R.K. (1985) Structural controls and mechanisms of diffusion in natural silicate melts. Contributions to Mineralogy and Petrology 89, 263-272.

Jambon A., Déruelle B., Dreibus G., and Pineau F. (1995) Chlorine and bromine abundance in MORB: the contrasting behaviour of the Mid-Atlantic Ridge and East Pacific Rise and implications for chlorine geodynamic cycle. Chemical Geology 126, 101-117.

Lecumberri-Sanchez P., Bodnar R.J. (2018) Halogen geochemistry of ore deposits: contributions towards understanding sources and processes. In: Harlov DE, Aranovich L (eds) The role of halogens in terrestrial and extraterrestrial geochemical processes: surface, crust, and mantle. Springer, Berlin, pp 261–305.

Louvel M., Cadoux A., Broocker R., Proux O. and Hazemann J.-L. (2020) New insights on Br speciation in volcanic glasses and structural controls on halogens degassing. American Mineralogist, in press, DOI: https://doi.org/10.2138/am-2020-7273.

Lowry, R.K., Hender,P., and Nolan,J.(1982)Tracer diffusion of some alkali, alkaline-earth and transition element ions in a basaltic and an andesitic melt, and the implications concerning melt structure. Contributions to Mineralogy and Petrology, 80,254–261

Luth R.W (1988) Raman spectroscopic study of the solubility mechanisms of F in glasses in the system CaO-CaF_2-SiO_2. American Mineralogist, 73, pp. 297-305

Lux G. (1987) The behavior of noble gases in silicate liquids: Solution, diffusion, bubbles and surface effects, with applications to natural samples. Geochimica et Cosmochimica Acta 51, 1549-1560.

Manning, D.A.C.(1981)The effect of fluorine on liquidus phase relationships in the system Qz–b–Or with excess water at 1 kb. Contributions to Mineralogy and Petrology , 76,206–215

McElroy M. B., Salawitch R. J., Wofsy S. C., and Logan J. A. (1986) Reductions of Antarctic ozone due to synergistic interactions of chlorine and bromine. Nature 321, 759-762.

Mysen, B, and Virgo,D. (1985) Iro, bearing silicate melts: relation between pressure and redox equilibria. Physics and Chemistry of Minerals 12, 191-200

Mysen, B.O, Cody, G.D. and Smith, A. (2004). Solubility mechanisms of fluorine in peralkaline and meta-aluminous silicate glasses and melts to magmatic temperatures. Geochimica et Cosmochimica Acta 68, 387-401.

Shewmon, P. (1963) Diffusion in solids. McGraw-Hill, New York, 1963, pp. 203

Shinohara H., Iiyama J.T., and Matsuo S. (1989) Partition of chlorine compounds between silicate melt and hydrothermal solutions. Geochimica et Cosmochimica Acta 53, 2617-2630.

Smith V.G., Tiller W.A. and Rutter, J.W. (1955) A mathematical analysis of soluteredistribution during solidification. Canadian Journal of Physics 33, 723–744.

Somogyi A., Drakopoulos M., Vincze L. , Vekemans B. , Camerani C. , Janssens K. , Snigirev A., and Adams F. (2001) ID18F: a new micro X-ray fluorescence end-station at the European Synchrotron Radiation Facility (ESRF): preliminary results. X-Ray Spectrometry 30, 242-252.

Vigneresse J.L. (2009) Evaluation of the chemical reactivity of the fluid phase through hard–soft acid–base concepts in magmatic intrusions with applications to ore generation. Chemical Geology 263:69–81

Villemant B., Caron B., Dubacq B. and Thierry P. (2017). Cl, Br and I behaviour during magma differentiation and degassing: contribution of a new LA-ICP-MS analysis technique. Goldschmidt 2017, Paris.

Wang L-X, Marks, M.A.W., Keller J., Markl, G. (2014) Halogen variations in alkaline rocks from the Upper Rhine Graben (SW Germany): Insights into F, Cl and Br behavior during magmatic processes. Chemical Geology 380, 133-144.

Webster J.D., Holloway J.R., and Hervig R.L. (1989) Partitioning of lithophile trace elements between H2O and H2O + CO2 fluids and topaz rhyolite melt. Econ Geol 84(1):116–134

Webster J.D., and Holloway J.R. (1990) Partitioning of F and Cl between magmatic hydrothermal fluids and highly evolved granitic magmas. Geological Society of America Special Paper 246:21–34

Webster J.D., Sintoni M.F., De Vivo B. (2009) The partitioning behavior of Cl, S, and H2O in aqueous vapor-±saline-liquid saturated phonolitic and trachytic melts at 200 MPa. Chemical Geology, 2009

Webster J.D., Baker D.R., and Aiuppa A. (2018) Halogens in mafic and intermediate-silica content magmas. In: Harlov DE, Aranovich L (eds) The role of halogens in terrestrial and extraterrestrial geochemical processes: surface, crust, and mantle. Springer, Berlin, pp 307–430

Widdifield C. M., Chapman R. P., and L., B. D. (2009) Chlorine, bromine, and iodine solid-state NMR spectroscopy. Annual Reports on Nuclear Magnetic Resonance Spectroscopy, 66, 195-326.

Yoshimura S. (2018) Chlorine diffusion in rhyolite under low-H_2O conditions. Chemical Geology, 483, 619–630.

Zeng Q. and Stebbins J.F. (2000) Fluoride sites in aluminosilicate glasses: high-resolution 19F NMR results American Mineralogist, 85, pp. 863-867

Figure captions

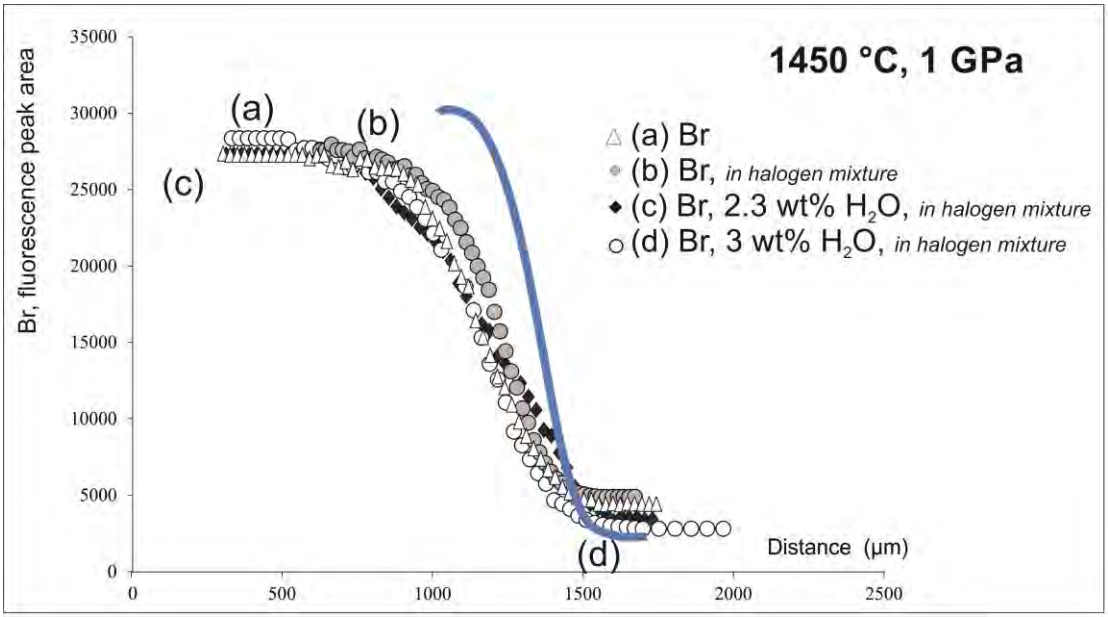

Figure 1

<u>Figure 1:</u> Br concentration profiles in halogen mixture obtained for K-rich phonolitic melts, at 1450°C and 1 GPa. The diffusion profiles of Br were measured using the SYXRF microprobe, ID18F, at the European Synchrotron Radiation Facility (ESRF, France) with a beam of 28 keV. In y axis, the Br concentrations is reported as florescence peak area. In the abscissa, the distance represents the distance along the diffusion profile, from the base of the Br-enriched half to the Br-poor half of the diffusion couple. Note that not all profiles begin at the base of the diffusion couple; the profile for the F-Cl-Br mixture was shortened to obtain the minimum number of points in the minimum analytical time. The calculated diffusion coefficients are

630 reported in Table 2. The zero-time experiment at 1350 °C is represented in solid blue line and
631 was obtained by SIMS measurement (CRPG, Nancy, France; Cadoux et al., 2017), with the Br-
632 poor plateau corresponding to 0 ppm and the Br-rich plateau corresponding to ~8000 ppm.

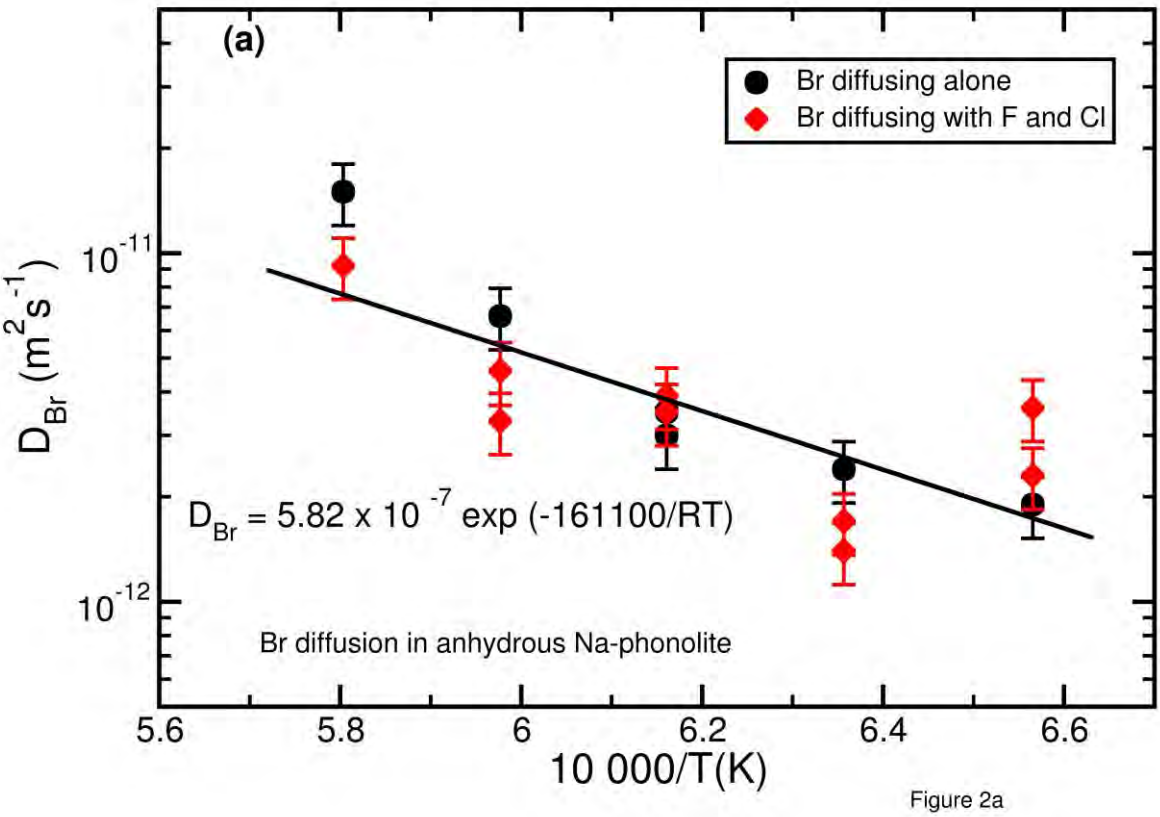

Figure 2a

633

This is a preprint, the final version is subject to change, of the American Mineralogist (MSA)
Cite as Authors (Year) Title. American Mineralogist, in press.
DOI: https://doi.org/10.2138/am-2020-7372

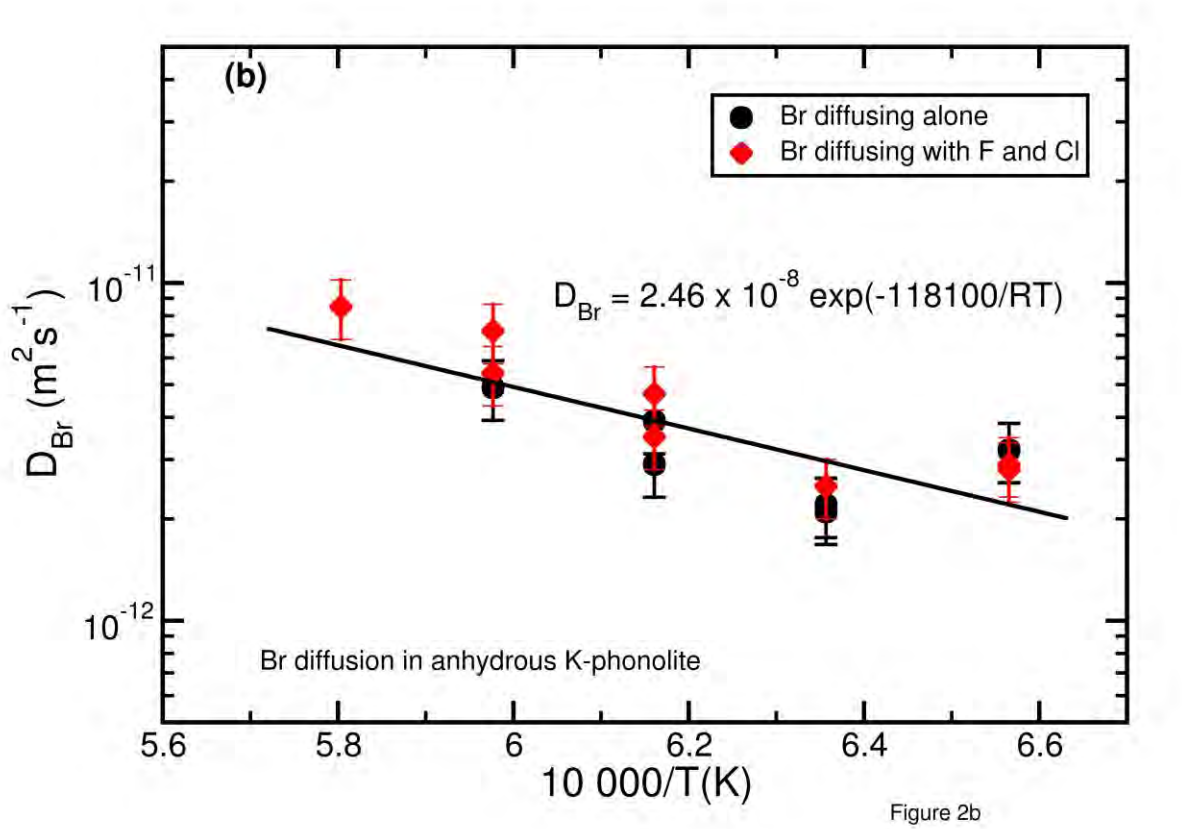

Figure 2: Arrhenius diagrams of Br diffusion coefficients for anhydrous Na- and K-rich phonolitic melts. (a) Data for Na-phonolite, (b) Data for K-phonolite. Anhydrous data are obtained with Br as the only diffusing halogen (in black) and with mixed halogen (F, Cl, Br) diffusion (in red). Experiments were performed at 1.0 GPa, under dry conditions, between 1250 °C and 1450 °C. The estimated uncertainty of the measurement is precised for each point (Table 3).

This is a preprint, the final version is subject to change, of the American Mineralogist (MSA)
Cite as Authors (Year) Title. American Mineralogist, in press.
DOI: https://doi.org/10.2138/am-2020-7372

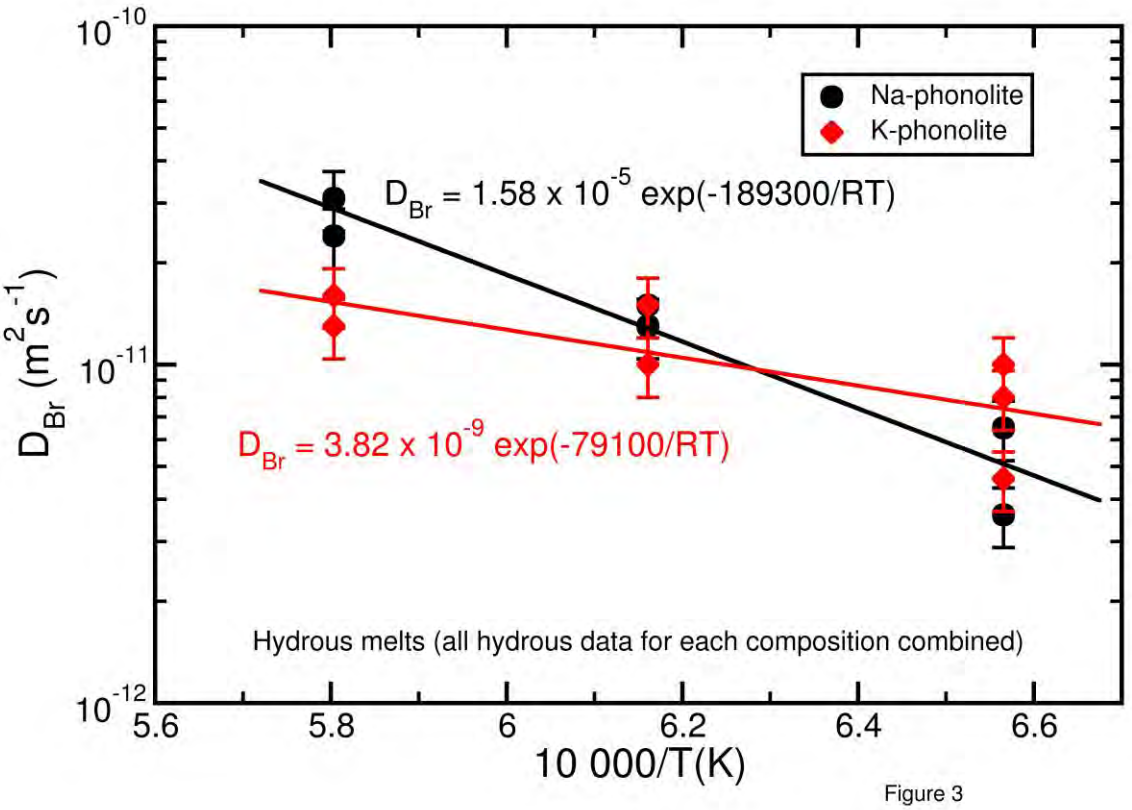

641

642 **<u>Figure 3:</u> Arrhenius diagram for Br diffusion coefficients in Na- and K-rich phonolitic**

643 **melts for hydrous conditions.**

644

This is a preprint, the final version is subject to change, of the American Mineralogist (MSA)
Cite as Authors (Year) Title. American Mineralogist, in press.
DOI: https://doi.org/10.2138/am-2020-7372

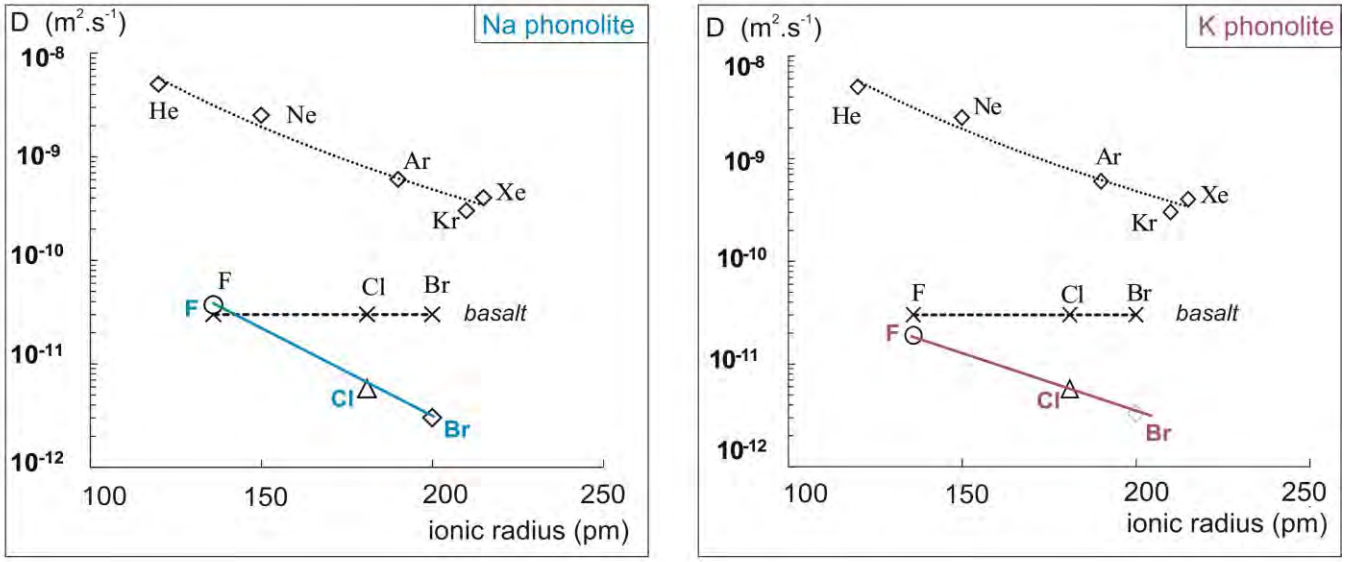

Figure 4: Halogen diffusion coefficient in phonolitic melts (Na on the left and K on the right) compared to noble gases in function of the ionic radius. The data for halogens are at 1350 °C and under anhydrous conditions for comparison to the data for basalt (Alletti et al. 2007).

This is a preprint, the final version is subject to change, of the American Mineralogist (MSA)
Cite as Authors (Year) Title. American Mineralogist, in press.
DOI: https://doi.org/10.2138/am-2020-7372

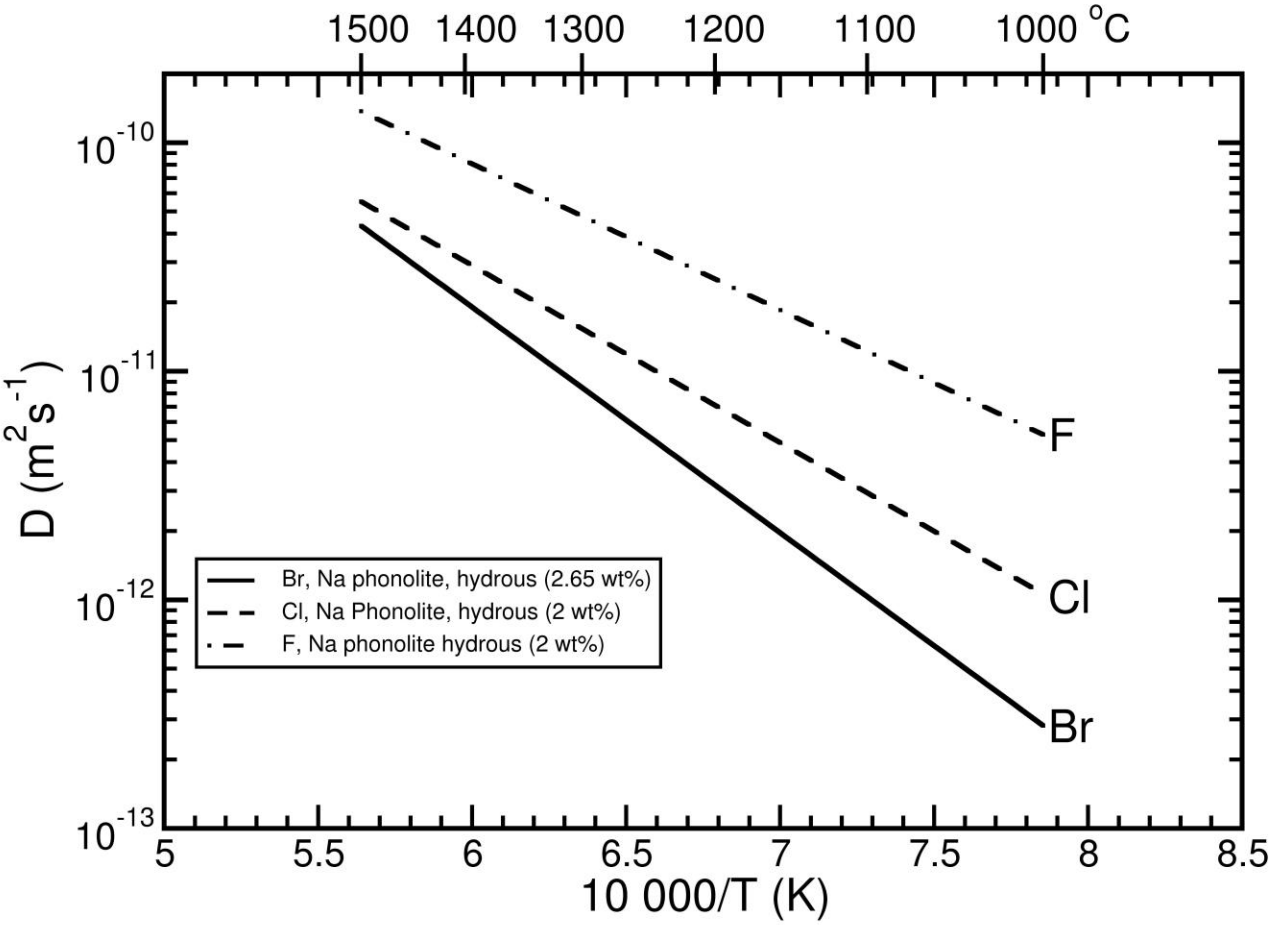

651

652 **Figure 5: Comparative halogen diffusion coefficient in Na-phonolitic hydrous melts.**

653 **Table captions**

654

655 **Table 1: Chemical compositions of the starting materials *("Anhydrous" composition).***
656 Average of 10 glass analyses by E.P.M.A.; in brackets: number of analyses. SD: standard
657 deviation of the oxide or halogen analyzed. LS: Laacher See, Na-rich Phonolite with LLST
658 corresponding to the first eruptive phase referred as "Lower Laacher See Tephra". Ves: Vesuvius,
659 K-rich Phonolite, with WP corresponding to the first eruptive phase referred as "White Pumice".
660 The LS and Ves starting materials display very similar Si/Al ratios (~2.2) but differ significantly
661 in their alkali ratio, by near a factor 4. The starting material is identical to previous experiments
662 for F and Cl diffusion (Balcone-Boissard et al. 2009). Br was measured after extraction by
663 pyrohydrolysis by ICP-MS following the analytical conditions described in Balcone-Boissard et
664 al. (2010). The Br-rich starting glass was measured by SIMS (See text for details)

665

666 **Table 2: Experimental conditions and diffusion coefficients.** 2a: Anhydrous conditions. 2b:
667 Hydrous conditions

668

669 **Table 3: Best fit parameters for the Arrhenius equation describing Br diffusion in Na- and**
670 **K- phonolitic melts.** The errors in the activation energy were calculated using the least squares
671 method.

672

673

674

675

Table 1

	LS LLST		Ves WP	
wt%	Avg (10)	*SD*	Avg (10)	*SD*
SiO_2	56.68	*0.34*	55.55	*0.39*
TiO_2	0.17	*0.07*	0.25	*0.08*
Al_2O_3	22.59	*0.21*	22.41	*0.2*
FeO	1.98	*0.11*	2.35	*0.22*
MnO	0.51	*0.08*	0.12	*0.11*
MgO	0.07	*0.02*	0.20	*0.02*
CaO	0.48	*0.06*	2.56	*0.09*
Na_2O	12.66	*0.17*	6.66	*0.07*
K_2O	4.86	*0.12*	9.88	*0.13*
Total	100		100	
F	0.42	*0.02*	0.27	*0.03*
Cl	0.19	*0.01*	0.33	*0.05*
Br	0.22	*0.3*	0.32	*0.2*
Na / K	2.3		0.6	
Si/Al	2.2		2.2	

Table 2a: Experimental conditions and diffusion coefficients for anhydrous phonolitic compositions

Na-rich phonolitic composition	T (°C)	P (GPa)	Time (s)	Counting time (s) ESRF	Nb traverses	D (m^2s^{-1})	D (m^2s^{-1})
Br diffusing alone							
HB-2007-20	1250	1	3600	10	1	1.9×10^{-12}	
HB-2007-22	1300	1	2400	10	1	2.4×10^{-12}	
HB-2007-19	1350	1	2400	10	1	3×10^{-12}	
HB-2007-25	1350	1	4800	10	1	3.5×10^{-12}	
HB-2007-24	1400	1	1200	10	1	6.6×10^{-12}	
HB-2007-21	1450	1	1200	10	1	1.5×10^{-11}	
Br diffusing with F and Cl							
HB-2007-20	1250	1	3600	10	1	2.3×10^{-12}	
HB-2007-43	1250	0.5	3600	10	1	3.6×10^{-12}	
HB-2007-22	1300	1	2400	10	2	1.7×10^{-12}	1.4×10^{-12}
HB-2007-19	1350	1	2400	10	1	3.9×10^{-12}	
HB-2007-25	1350	1	4800	10	1	3.5×10^{-12}	
HB-2007-24	1400	1	1200	10	1	4.6×10^{-12}	
HB-2007-24	1400	1	1200	30	1	3.3×10^{-12}	
HB-2007-21	1450	1	1200	10	1	9.2×10^{-12}	

K-rich phonolitic composition	T (°C)	P (GPa)	Time (s)	Counting time (s) ESRF	Nb traverses	D (m^2s^{-1})	D (m^2s^{-1})
Br diffusing alone							
HB-2007-20	1250	1	3600	10	1	3.2×10^{-12}	
HB-2007-22	1300	1	2400	10	2	2.1×10^{-12}	2.2×10^{-12}
HB-2007-19	1350	1	2400	10	1	2.9×10^{-12}	
HB-2007-25	1350	1	4800	10	1	3.9×10^{-12}	
HB-2007-24	1400	1	1200	10	1	4.9×10^{-12}	
HB-2007-21	1450	1	1200	10	1	nd	
Br diffusing with F and Cl							
HB-2007-19	1250	1	3600	10	1	2.8×10^{-12}	
HB-2007-45	1250	0.5	3600	10	1	2.9×10^{-12}	
HB-2007-22	1300	1	2400	10	1	2.5×10^{-12}	
HB-2007-19	1350	1	2400	10	1	4.7×10^{-12}	
HB-2007-25	1350	1	4800	10	1	3.5×10^{-12}	
HB-2007-24	1400	1	1200	10	1	5.4×10^{-12}	
HB-2007-23	1400	1	1200	30	1	7.2×10^{-12}	
HB-2007-21	1450	1	1200	10	1	8.5×10^{-12}	

Table 2b: Experimental conditions and diffusion coefficients for hydrous phonolitic compositions

	T (°C)	P (GPa)	Time (s)		Nb traverses	D (m^2s^{-1}) Br	D (m^2s^{-1})
Na-rich phonolitic composition with 2.3 wt%H_2O							
HB-2007-42	1250	1	1500	10	1	3.6×10^{-12}	
HB-2007-41	1350	1	1200	10	1	1.5×10^{-11}	
HB-2007-40	1450	1	800	10	1	2.4×10^{-11}	
Na-rich phonolitic composition with 3 wt%H_2O							
HB-2007-34	1250	1	1200	10	1	6.5×10^{-12}	
HB-2007-38	1350	1	800	10	1	1.3×10^{-11}	
HB-2007-39	1450	1	400	10	1	3.1×10^{-11}	
K-rich phonolitic composition with ~2.3 wt%H_2O							
HB-2007-42	1250	1	1500	10	1	4.6×10^{-12}	
HB-2007-41	1350	1	1200	10	1	1×10^{-11}	
HB-2007-40	1450	1	800	10	2	1.6×10^{-11}	1.3×10^{-11}
K-rich phonolitic composition with 3 wt%H_2O							
HB-2007-34	1250	1	1200	10	2	1×10^{-11}	8×10^{-12}
HB-2007-38	1350	1	800	10	1	1.5×10^{-11}	
HB-2007-39	1450	1	400	10	1	nd	

nd not determined

Table 3

Na-rich phonolitic melt	D_0 (m^2s^{-1})	Uncertainty+	Uncertainty-	Ea (kJ mol^{-1})	Uncertainty	$\%H_2O$
Br anhydrous melt	5.8×10^{-7}	1.6×10^{-5}	1.9×10^{-6}	161	38.6	0
Br hydrous melt	1.6×10^{-5}	1.0×10^{-4}	1.4×10^{-5}	189	27.0	2.65

K-rich phonolitic melt	D_0 (m^2s^{-1})	Uncertainty+	Uncertainty-	Ea (kJ mol^{-1})	Uncertainty	$\%H_2O$
Br anhydrous melt	2.5×10^{-8}	2.2×10^{-7}	3.0×10^{-8}	118	26.9	0
Br hydrous melt	3.8×10^{-9}	5.8×10^{-7}	1.6×10^{-8}	79	27.0	2.65